Proton NMR Study of the Molecular and Electronic Structure of Ferric Chlorin Complexes: Evidence for π Bonding by the Orbital Derived from the Porphyrin a_{1u} Orbital

Silvia Licoccia,[1] Mariann J. Chatfield, Gerd N. La Mar,* Kevin M. Smith, Kathryn E. Mansfield, and R. R. Anderson

Contribution from the Department of Chemistry, University of California, Davis, California 95616. *Received August 26, 1988*

Abstract: The proton NMR spectra of a variety of low-spin and high-spin ferric complexes of the naturally occurring chlorin derivative pyropheophorbide *a* methyl ester have been recorded and assigned. The complete assignments for the low-spin, dicyano complex were effected by a combination of partial isotope labeling, paramagnetic relaxation, multiplet structure, and nuclear Overhauser measurements in viscous solvent. The resulting contact shift pattern reflects π spin delocalization into both the highest filled MO equivalent to the porphyrin $3e_\pi(xz,yz)$, as well as into the former a_{1u} orbital of the porphyrin. The saturation of a pyrrole ring to produce a chlorin is concluded to uniquely stabilize the orbital ground state of the iron, which allows the lone spin to π bond to the two unmodified *trans*-pyrroles. The pattern of contact shift asymmetry of the pyrroles adjacent to the saturated ring provides a potential model for interpreting NMR spectra of iron chlorin enzymes. Ferric pyropheophorbide *a* methyl ester yields a six-coordinate high-spin complex in dimethyl sulfoxide in both the presence and absence of chloride, indicating that high-spin ferric chlorins have a greater affinity for weak-field ligands than do analogous porphyrins. The $\sim 10^3$ acceleration of the rate of macrocycle "inversion" of pyropheophorbide-iron chloride, as induced by associative halide exchange, supports a more flexible core for chlorins relative to porphyrins.

Iron chlorins of different forms exist in a wide variety of naturally occurring enzymes[2-6] or can be formed from heme proteins under suitable conditions.[7-10] While the special role of chlorins relative to porphyrins is understood in their dominant role in photosynthetic reaction centers,[11,12] the properties of chlorins relevant to their enzymatic functions are more obscure. Both structural[13,14] and limited ligand binding[13,15] studies on model compounds have indicated relatively conserved properties for chlorins and porphyrins. With respect to bonding to metals, one prominent difference proposed[16,17] for chlorins and porphyrins is that the former has a filled π MO capable of, and energetically ideally situated for, π interaction with iron d orbitals, which is symmetry-restricted (a_{1u}) from such interaction in porphyrins.

Nuclear magnetic resonance, NMR, has played a key role in the characterization of electronic and molecular structural, dynamic, and functional properties of heme-containing proteins[18] and hence can be expected to play a similar role in elucidating iron-chlorin containing enzymes. This is particularly true in paramagnetic derivatives where the hyperfine interactions not only lead to resolution of the prosthetic group proton signals in large proteins but also provide direct information on the nature of the metal-macrocycle bonding.[18-21] The ^{1}H NMR spectra of several such paramagnetic chlorin proteins have been reported[4,6] but could not be interpreted. As in the case for porphyrins, the interpretation of NMR spectral parameters in intact chlorin-containing proteins is considerably facilitated by initial studies on appropriate chlorin model compounds.[19-21]

Several ^{1}H NMR studies of iron complexes of synthetic chlorins have been reported that have suggested both some differences and similarities to analogous porphyrin complexes.[14,22-24] However, definitive assignments are lacking, as are needed substituents as spectral probes,[20,25] and the detailed studies to date have been restricted largely to the unligated iron(II) system.[14,22,26] A more recent study on five-coordinate, ferric complexes of synthetic chlorins suggests[24] only small differences in contact shift patterns from that of porphyrins, but the multitude of spin delocalization mechanisms[19-21] for high-spin iron(III) make this less than an ideal case for detailed probing of π-bonding properties of chlorins. The ideal oxidation/spin state for this purpose is low-spin iron(III), which not only exhibits advantageous spectral resolution but also has the lone iron spin symmetry restricted to π spin delocalization.[19-21]

To provide NMR spectral information of potential direct relevance to native enzymes, we select for study here the iron

* Address correspondence to this author.

(1) On leave from the Department of Chemical Sciences and Technologies, II Universita' di Roma Tor Vergata, 00173 Rome, Italy.

(2) Siegel, L. M., Singer, T. P., Ondarza, R. N., Eds. *Mechanisms of Oxidizing Enzymes*; Elsevier: New York, 1978; pp 201-213, and references therein.
(3) Davis, J. C.; Averill, B. A. *J. Biol. Chem.* **1981**, *256*, 5992-5996.
(4) Ikeda-Saito, M.; Inubushi, T. *FEBS Lett.* **1987**, *214*, 111-116.
(5) Wharton, D. C.; Wintraub, S. T. *Biochem. Biophys. Res. Commun.* **1980**, *97*, 236-242.
(6) Timkovich, R.; Cork, M. S. *Biochemistry* **1982**, *21*, 5119-5123.
(7) Berzofsky, J. A.; Peisach, J.; Horecker, B. L. *J. Biol. Chem.* **1972**, *247*, 3783-3791.
(8) Chatfield, M. J.; La Mar, G. N.; Lecomte, J. T. J.; Balch, A. L.; Smith, K. M.; Langry, K. C. *J. Am. Chem. Soc.* **1986**, *108*, 7108-7110.
(9) Chatfield, M. J.; La Mar, G. N.; Smith, K. M.; Leung, H.-K.; Pandey, R. K. *Biochemistry* **1988**, *27*, 1500-1507.
(10) Bondoc, L. L.; Chau, M.-H.; Price, M. A.; Timkovich, R. *Biochemistry* **1986**, *25*, 8458-8466.
(11) Clayton, R. K.; Sistrom, W. R., Eds. *The Photosynthetic Bacteria*; Plenum Press: New York, 1978.
(12) Diesenhofer, J.; Epp, O.; Miki, K.; Huber, R.; Michel, H. *J. Mol. Biol.* **1984**, *180*, 385-397.
(13) Strauss, S. H.; Silver, M. E.; Ibers, J. A. *J. Am. Chem. Soc.* **1983**, *105*, 4108-4109.
(14) Strauss, S. H.; Silver, M. E.; Long, K. M.; Thompson, R. G.; Hudgens, R. A.; Spartalian, K.; Ibers, J. A. *J. Am. Chem. Soc.* **1985**, *107*, 4207-4215.
(15) Strauss, S. H.; Holm, R. H. *Inorg. Chem.* **1982**, *21*, 863-868.
(16) Hanson, L. K.; Chang, C. K.; Davis, M. S.; Fajer, J. *J. Am. Chem. Soc.* **1981**, *103*, 663-670.
(17) Chang, C. K.; Hanson, L. K.; Richardson, P. F.; Young, R.; Fajer, J. *Proc. Natl. Acad. Sci. U.S.A.* **1981**, *78*, 2652-2656.
(18) Satterlee, J. D. *Annu. Rep. NMR Spectrosc.* **1986**, *17*, 79-178.
(19) La Mar, G. N.; Walker (Jensen), F. A. *The Porphyrins* **1978**, *4B*, 61-157.
(20) La Mar, G. N. In *Biological Applications of Magnetic Resonances*; Shulman, R. G., Ed.; Academic Press: New York, 1979; pp 305-343.
(21) Goff, H. In *Iron Porphyrins*; Lever, A. B. P., Gray, H. B., Eds.; Addison-Wesley: Reading, MA, 1983; Part, I, pp 237-281.
(22) Strauss, S. H.; Pawlik, M. J. *Inorg. Chem.* **1986**, *25*, 1921-1923.
(23) Strauss, S. H.; Pawlik, M. J.; Skowyra, J.; Kennedy, J. R.; Anderson, O. P.; Spartalian, K.; Dye, J. L. *Inorg. Chem.* **1987**, *26*, 724-730.
(24) Pawlik, M. J.; Miller, P. K.; Sullivan, E. P.; Levstik, M. A.; Almond, D. A.; Strauss, S. H. *J. Am. Chem. Soc.* **1988**, *110*, 3007-3012.
(25) La Mar, G. N. In *NMR of Paramagnetic Molecules*; La Mar, G. N., Horrocks, Jr., W. D., Holm, R. H., Eds.; Academic Press: New York, 1973; pp 86-123.

0002-7863/89/1511-6087$01.50/0

derivative of chlorophyll *a*,[24] (pyropheophorbide *a* methyl ester)iron(III), **1** (which we abbreviate PyropheoMEFe[III]). The

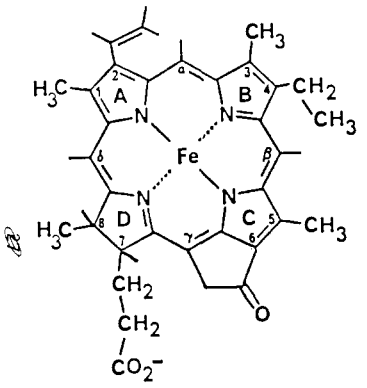

1

absence of any symmetry for this derivative leads to large numbers of peaks (22 expected under optimal conditions) and a necessarily complicated NMR spectrum, and general routes to isotope labeling for more than a very few sites have not been developed.[28] However, we have shown that for the important low-spin ferric complexes, complete and unambiguous resonance assignments, as well as stereochemistry determination, are possible based solely on the nuclear Overhauser effect,[29] NOE, *if carried out in viscous solvents*.[30,31] This is due to the important ^1H–^1H cross relaxation being selectively enhanced by immobilization while the paramagnetic ^1H relaxation is unchanged. Thus the complete structure of the extracted prosthetic group of sulfmyoglobin,[7-10] **2**, could be established[31] on the basis of such NOE studies.

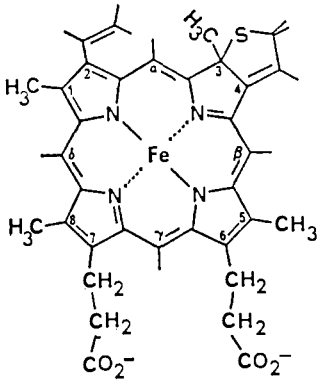

2

We demonstrate herein that the low-spin, dicyano complex PyropheoMEFe$(CN)_2^-$ indeed exhibits direct evidence for important contributions to π bonding for the former a_{1u} ligand orbital[16,17] and that the resulting contact shift pattern[19-21] deduced from the present complex **1** and that of the sulfmyoglobin extract,[31] **2**, provides a model for interpreting the NMR spectra of some iron chlorin enzymes.[4] Partial assignments of a variety of high-spin complexes of PyropheoMEFe(III) on the basis of partial deuteration and relaxation time measurements give evidence for both structural and dynamic properties that are distinct from their porphyrin counterparts.

Experimental Section

Sample Preparation. Pyropheophorbide *a* methyl ester was obtained by degradation of chlorophyll *a*[27] isolated from *Spirulina maxima* algae.[32] Iron insertion was accomplished by the ferrous chloride method.[33] The iron complex, **1**, is abbreviated PyropheoMEFe(III). The derivative deuterated at 5-methyl, δ-meso, and γ-meso positions was prepared as previously described;[28,34] impurities obscured the ^1H NMR spectral window between 0 and 6 ppm. Pyropheophorbide solutions were prepared by adding the appropriate solvent to the complex under a nitrogen atmosphere.

The high-spin bis(DMSO) complex was prepared by dissolution of **1** in $(C^2H_3)_2SO$, and chloride impurities were removed by titration with 0.1 M $AgNO_3$ and subsequent filtering of the AgCl precipitate to produce the six-coordinate product[35] (λ_{max} = 690, 615, 410 nm). The five-coordinate high-spin chloro complex was obtained by dissolution of the pyropheophorbide, **1**, in C^2HCl_3 (λ_{max} = 630, 390 nm). The iron chloride complex in dimethyl sulfoxide was prepared by dissolving the hemin in $(C^2H_3)_2SO$, followed by the addition of excess tetraethylammonium chloride. The optical spectrum of this complex (λ_{max} = 745, 690, 410 nm) is distinct from either the bis(DMSO) or the C^2HCl_3 monochloride complex, in contrast with similarly treated iron porphyrin complexes.[35]

Imidazole complexes of **1** were prepared by the addition of at least 4 equiv of imidazole (Aldrich), (1,2-$^2H_2$)imidazole (MSD), or ($^2H_4$)-imidazole (MSD) to the bis(DMSO) complex followed by equilibration at 22 °C for 12 h; approximately 5% of the complex remains as the bis(DMSO) product under these conditions. Unlike the rapidly ligating porphyrin counterparts, the addition of smaller amounts of imidazole or failure to equilibrate the pyropheophorbide solutions resulted in only small quantities of the bis(imidazole) product, with the remaining products occurring as bis(DMSO). No evidence for the formation of mono(imidazole) complexes was observed (see text).

Low-spin cyanide complexes were prepared in a variety of solvents, according to the experimental requirements. Although spectra were observable in $(C^2H_3)_2SO$ solutions, for ^1H NMR spin decoupling, **1** was dissolved in $C^2H_3O^2H$, which greatly increased spectral resolution, in the presence of 25% $(C^2H_3)_2SO$ (which slowed sample decomposition) and 2 equiv of KCN. The addition of less than 2 equiv of cyanide produces a mixture of bis(DMSO) and dicyano complexes, confirming the bis-ligation of cyanide. Since chemical shifts were invariant upon 3-fold dilution, the species are assumed to be monomeric.

Nuclear Overhauser enhancements, NOEs, are generally not detectable for paramagnetic hemins in standard solvents at 25 °C. Hence, for NOE studies, solutions were prepared in mixtures of 2:1 $(C^2H_3)_2SO/^2H_2O$ in the presence of 2 equiv of KCN and observed at −20 °C, where the solvent viscosity[36] places the molecular tumbling rate into the slow-motion limit and significantly increases the cross-relaxation rate, rendering observable negative NOEs.[30,31]

Optical Spectra. Optical spectra were observed at ambient temperatures on a Hewlett-Packard 8540A UV-vis spectrophotometer using 1-cm light-path quartz cells following dilution of 10 μL of 1–5 mM **1** into 2 mL of solvent in the optical cell. Sample purity was determined by analysis of the corresponding ^1H NMR spectrum.

NMR Spectra. A Nicolet NTC-360 spectrometer operating in the quadrature mode was used to obtain 360-MHz ^1H NMR spectra. Typical spectra consisted of 1024 transients of 8192 data points over a 50-kHz (low-spin) or 140-kHz (high-spin) bandwidth using a 6.5-μs 90° pulse. All chemical shifts are given in ppm from 2,2-dimethyl-2-silapentane-5-sulfonate (DSS) referenced against residual solvent signals. Pyropheophorbide solutions were 1–5 mM.

^1H decoupling was observed over a 16-kHz bandwidth centered according to the irradiated and decoupled frequencies. Nonselective spin-lattice relaxation rates were obtained by using the standard (180°-τ-90°) inversion-recovery method with a composite 90° pulse and a repetition rate of 2 s^{-1}. T_1 relaxation times were calculated from semilogarithmic plots prepared from spectra consisting of 256 scans. NOE spectra were recorded at −20 °C on dicyanopyropheophorbide dissolved in 2:1 $(C^2H_3)_2SO/^2H_2O$ (viscosity ~10 cP[36]) by application of a 30-ms presaturation pulse with the decoupler on-resonance; corresponding reference spectra were collected with the decoupler off-resonance. On- and off-resonance spectra were alternated every 128 scans to give a total of 8000

(26) Strauss, S. H.; Long, K. M.; Magerstädt, M.; Gansow, O. *Inorg. Chem.* **1987**, *26*, 1185–1187.
(27) Kenner, G. W.; McCombie, S. W.; Smith, K. M. *J. Chem. Soc., Perkin Trans. 1* **1973**, 2517–2523.
(28) Fajer, J.; Fujita, I.; Davis, M. S.; Forman, A.; Hanson, L. K. *Adv. Chem. Ser.* **1982**, *201*, 489–513.
(29) Noggle, J. H.; Schirmer, R. E. *The Nuclear Overhauser Effect*; Academic Press: New York, 1971.
(30) Yu, C.; Unger, S. W.; La Mar, G. N. *J. Magn. Reson.* **1986**, *67*, 346–350.
(31) Chatfield, M. J.; La Mar, G. N.; Parker, Jr., W. O.; Smith, K. M.; Leung, H.-K.; Morris, I. K. *J. Am. Chem. Soc.* **1988**, *110*, 6352–6358.
(32) Smith, K. H.; Goff, D. A.; Simpson, D. J. *J. Am. Chem. Soc.* **1985**, *107*, 6946–6954.
(33) Smith, K. M.; Fujinari, E. M.; Langry, K. C.; Parish, D. W.; Tabba, H. D. *J. Am. Chem. Soc.* **1983**, *105*, 6638–6646.
(34) Smith, K. M.; Bobe, F. W.; Goff, D. A.; Abraham, R. J. *J. Am. Chem. Soc.* **1986**, *108*, 1111–1120.
(35) Budd, D. L.; La Mar, G. N.; Langry, K. C.; Smith, K. M.; Nayyir-Mazhir, R. *J. Am. Chem. Soc.* **1979**, *101*, 6091–6096.

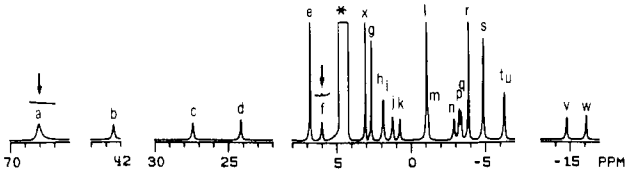

Figure 1. The 360-MHz ^1H NMR spectrum of (dicyano pyropheophorbide methyl ester)iron(III) in 2:1 $(C^2H_3)_2SO/^2H_2O$ at 25 °C. Resonances are labeled a to w from left to right. An asterisk marks the solvents residual signals. Different portions have constant horizontal and vertical scales. Inserts with vertical arrows show the effect of deuteration at 5-C^2H_3 and δ-meso-^2H.

scans with a repetition rate of 0.7 s^{-1}. Difference spectra were computer corrected to eliminate off-resonance effects (see Figure 2). The concentration independence of T_1's at both 25 and −20 °C confirms the monomeric nature of the complexes.

^2H NMR spectra were recorded on a Nicolet NT-500 spectrometer with a deuterium probe operating at a frequency of 76.76 MHz. These spectra were collected on 4096 data points over a 10-kHz bandwidth with a 90° pulse of 25 μs and consisted of 1000 transients.

Results

Low-Spin Complexes. Macrocyclic Assignments. The 360-MHz ^1H NMR trace of PyropheoMeFe$(CN)_2^-$ at 25 °C is illustrated in Figure 1 and reveals 20 resolved resonances attributable to the complex; 22 peaks are expected based on the structure **1**. All labeled peaks except the sets a, e, g, l, r, s, and h, i, and t, u exhibit single proton intensity; the first set must arise from methyls; h, i and t, u sets each consist of two accidentally degenerate single-proton peaks that are resolved upon deconvolution and at other temperatures (see below). Thus all expected 22 nonequivalent sets of protons are detected. The nonselective T_1's for all resonances were determined by the inversion-recovery technique, and the T_1 values are listed in Table I. On the expectation that the meso positions are closest to the iron, we tentatively attribute the three peaks with the shortest T_1's, f, i, and k, to the three meso-H's. Conversely, one methyl peak, g, exhibits a T_1 over twice that of any other peak and can be assigned to the 7-propionate methoxyl ester. A single isotope-labeled derivative could be prepared[28,34] with simultaneous deuteration of 5-C^2H_3, γ-meso-C^2H_2 and δ-meso-^2H. Its dicyano complex clearly identifies a as 5-CH_3 and b as δ-meso-H (inset to figure indicated by arrows); impurities obliterate the region 1–6 ppm where the other two positions must resonate (not shown).

Resolved multiplets and spin-decoupling provide additional assignments; relevant expanded portions of the trace are shown in Figure 2 in the supplementary material (see the paragraph at the end of the article). A triplet for l identifies it as 4-β-CH_3, and decoupling l leads to simplification of the complex multiplicity of p,q to an A–B doublet of ~14 Hz assigning p,q to the 4-α-CH_2. Irradiating the composite t,u leads to similar simplification to a ~14-Hz A–B doublet of m and n and identifies t,u and m,n as 7-propionate CH_2-CH_2. Methyl peak s fails to exhibit resolvable multiplet structure but exhibits detectable narrowing in the difference spectrum upon irradiating c; hence, c and s must arise from 8-H and 8-CH_3 (the only other methyl that is expected to experience spin–spin splittings). The 2-vinyl $H_{\beta t}$, peak v, is identified by its resolved ~16-Hz doublet structure, which, upon decoupling b, collapses (and peak w narrows); hence, a, v, and w arise from 2-H_α, 2-$H_{\beta t}$, and 2-$H_{\beta c}$, respectively.

Since detectable NOEs in small paramagnetic complexes require a viscous solvent to increase cross relaxation,[30,31] we carry out NOEs at −20 °C where the viscosity is ~10 times[36] that at 25 °C. Peak identities at 25 and −20 °C are connected by variable-temperature studies, and the resulting apparent intercepts at $T^{-1} = 0$ of Curie plots (shift versus T^{-1}) are indicated in Table I. The straight lines of the Curie plots, the reasonable intercepts, and the concentration-independent shifts at −20 °C confirm a largely monomeric complex in solution.

(36) Schichman, S. A.; Amey, R. L. *J. Phys. Chem.* **1971**, *75*, 98–102.

Table I. Spectral Properties of (Dicyanopyropheophorbide methyl ester)iron(III) in 2:1 $(C^2H_3)_2SO/^2H_2O$ at 25 °C

assignment	label[a]	$\Delta H/H$,[b] ppm	intercept[c]	10^{-1} T_1, ms	hyperfine shift[d]
1-CH_3	e	6.74	2.9	6.0	3.5
2-Hα	b	42.80	4.9	4.8	34.8
2-$H_{\beta trans}$	v	−14.99	15.1	9.8	−20.9
2-$H_{\beta cis}$	w	−16.32	16.4	5.6	−22.3
3-CH_3	r	−3.93	6.6	14.0	−7.1
4-α-CH_2	p	−3.26	6.2	9.8	−6.9
	q	−3.40	5.9	10.0	−7.1
4-β-CH_3	l	−1.09	2.2	15.7	−2.7
5-CH_3	a	68.50	−13.3	2.1	65.3
7-H	d	24.28	7.1	4.6	20.1
7-α-CH_2	t	−6.36	3.3	4.5	−8.5
	u				
7-β-CH_2	m	−1.22	1.5	5.2	−3.6
	n	−3.05	6.0	2.5	−5.5
ester OCH_3	g	3.02	3.5	36.0	−0.6
8-H	c	27.74	−1.5	2.8	23.6
8-CH_3	s	−4.87	2.3	4.2	−6.5
α-meso-H	k	0.40	9.7	1.9	−8.8
β-meso-H	i	1.67	12.9	1.9	−7.7
γ-meso-CH_2	h	2.05	11.2	5.0	−2.3
	j	1.37	11.8	4.8	−2.9
δ-meso-H	f	5.56	4.8	1.3	−2.8

[a] Labeled as in Figure 1. [b] In ppm from DSS. [c] Apparent intercept at $T^{-1} = 0$ in plot of $\Delta H/H$ versus reciprocal absolute temperature. [d] Observed shift referenced to the diamagnetic Mg(II) complex.[49]

The trace of PyropheoMEFe$(CN)_2^-$ at −20 °C is shown in Figure 3A. Saturating c (8-H) gives the expected NOE to s (8-CH_3), as well as NOEs to m and to one of the components of t,u (Figure 3B), which belongs to the neighboring 7-propionate (see above). Saturating d leads to sizeable NOEs to the composite t,u and smaller NOEs to s (8-CH_3), h, and j (Figure 3C). Spin decoupling d also perturbs t,u (not shown), so d must arise from 7-H and t,u from 7-α-CH_2; this assigns m,n to 7-β-CH_2. The peaks in the window 0–5 ppm must then originate from meso-H's and γ-meso-CH_2; hence the NOEs to h and j suggest they arise from the adjacent γ-meso-CH_2 of the exocyclic ring (see below).

Saturation of peak i (computer corrected for off-resonance saturation of h) yields NOEs only to a (5-CH_3) and p,q (4-α-CH_2), uniquely assigning i to β-meso-H (Figure 3D). Irradiating peak k (computer corrected for off-resonance saturation of i) yields NOEs solely to methyl peak r and peak b (2-H_α) (Figure 3E), which dictates that k is α-meso-H and r is 3-CH_3. The expected NOE between p,q (4-α-CH_2) and r (3-CH_3) is detected (not shown). In Figure 3F, saturating f (δ-meso-H) yields an NOE to e, the only unassigned methyl, which must be 1-CH_3, and to c (8-H) and hence confirms f as δ-meso-H. The expected NOE from f (δ-meso-H) to s (8-CH_3) is not observed because of the more rapid relaxation of s (see Table I) and a slightly larger distance from δ-meso-H. The assignment of r to 1-CH_3 is confirmed by detecting the expected NOE to both b (2-H_α) and v (2-$H_{\beta t}$) (not shown). The observation of large NOEs between peaks h and j (Figure 3G,H) confirms their geminal nature, and the NOEs to solely 7-position substituents, d (7-H) and t,u (7-α-CH_2) confirm them as γ-meso-CH_2. The resulting complete assignments are summarized in Table I.

Axial Ligand Assignments. The 360-MHz ^1H NMR trace of the bis(imidazole) (Im, **3**) complex, PyropheoMEFe$(Im)_2^+$, is illustrated in Figure 4A. Except for the two broad upfield peaks

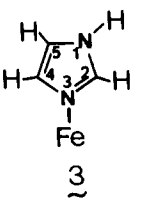

3

a′, b′ (with intensity consistent with each arising from a single proton), the number of peaks, their relative intensities, and their

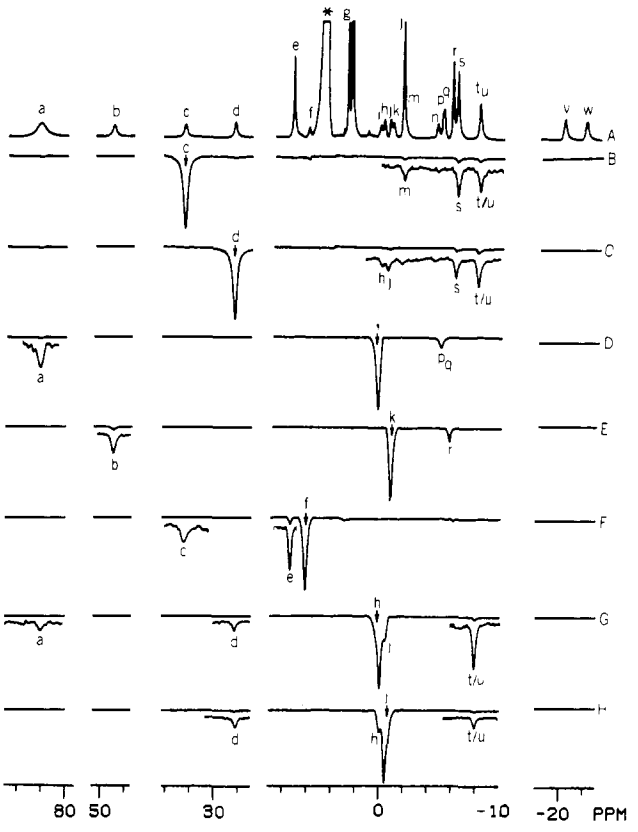

Figure 3. Resonance assignments of the dicyano complex of **1** by NOE. (A) the 360-MHz ^{1}H NMR spectrum of (dicyanopyropheophorbide methyl ester)iron(III) in 2:1 $(C^2H_3)_2SO/^2H_2O$ at −20 °C. Resonances are labeled a to w as in Figure 1 and have been connected to the 25 °C spectrum through variable-temperature experiments. NOE difference spectra: (B) irradiation of the 8-H (peak c) yields an NOE to the 8-CH_3 (peak s) and to the propionate peaks t/u; hence t/u must be the 7α-CH_2. (C) Irradiation of peak d yields NOEs to the assigned 7α-CH_2 (peaks t/u) and 8-CH_3 (peak *s*); hence d is due to the 7-H. (D) Irradiation of peak i yields NOEs to the 5-CH_3 (peak a) and to the 4α-CH_2 (peaks p, q), thus assigning peak i as the β-meso-H. (E) Saturation of peak k (α-meso-H) gives NOEs to the 2-Hα (peak b) and to peak r which is thus identifed as the 3-CH_3. Spectra for both traces D and E were computer-corrected to eliminate off-resonance effects from peaks h and j. (F) Irradiation of the δ-meso-H (peak f) yields an NOE to peak e, identifying it as the 1-CH_3, together with an expected NOE to the 8-H (peak c). (G, H) Peaks h and j yield, upon saturation, reciprocal NOEs and both show connectivity with the 7-H (peak d) and the 7α-CH_2 (peaks t/u); peaks h and j are thus identified as the γ-meso-CH_2. Note that for both spectra the reference frequencies were chosen to be symmetrical with respect to j and h: the NOEs thus obtained are real and indicative of geminal partners. Moreover, the spectra were computer-corrected for off-resonance effects due to k and i.

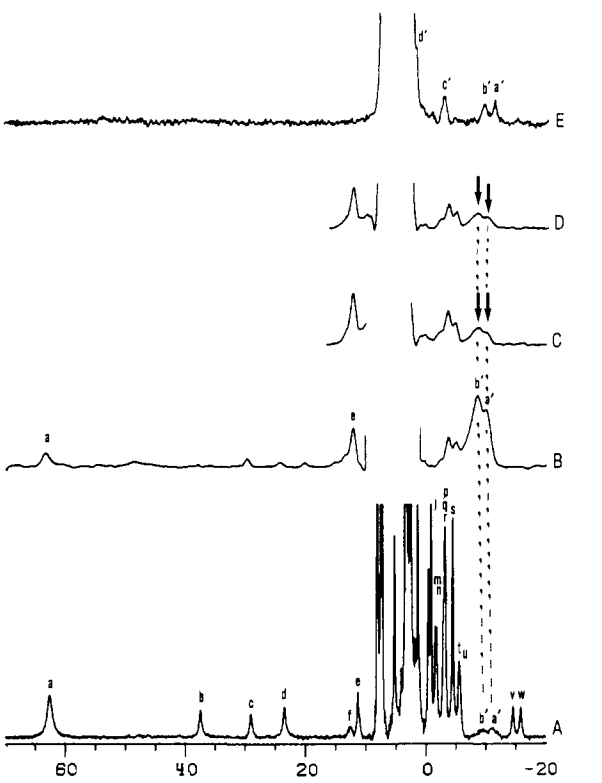

Figure 4. (A) The 360-MHz ^{1}H NMR spectrum of (bis(imidazole)-pyropheophorbide methyl ester)iron(III) in $(C^2H_3)_2SO$ at 25 °C. The same labeling used in Figure 1 for the dicyano derivative has been used because of the similarity in intensity, line width, and chemical shifts of the resonances. The only new nonlabile proton peaks are labeled a′ and b′, and both have a single proton intensity. (B) ^{1}H NMR spectrum of the same solution giving rise to trace A obtained using the WEFT pulse sequence[38] showing enhancement of peaks a′ and b′ due to rapid relaxation. With the exception of 5-CH_3 (peak a) and 1-CH_3 (peak e), any other fast-relaxing protons must resonate in the region obscured by the solvent. (C) WEFT spectrum of the complex obtained from per-deuterated $^2H_4$-imidazole. Both a′ and b′ show loss of intensity; hence they arise from the coordinated imidazole. (D) WEFT spectrum of the derivative obtained by using *1,2*-($^2H_2$)-imidazole. Again both a′ and b′ show loss of intensity due to deuteration: hence they both arise from the imidazole 2-H's. The distinction between them is attributed to the asymmetry of the chlorin ligand. (E) The 76.76-MHz ^{2}H NMR spectrum of (bis[($^2H_4$)imidazole]pyropheophorbide methyl ester)iron(III) in $(CH_3)_2SO$ at 25 °C showing direct deuterium detection. Because of its longer relaxation time with respect to a′ and b′, peak c′ must be further away from the iron and is thus assigned to the two imidazole 5-^{2}H's. The only other detected signal is peak d′, appearing as a shoulder on the strong solvent resonance, which is assigned to the two imidazole 4-^{2}H's.

chemical shifts[37] are very similar to those of PyropheoMEFe-$(CN)_2^-$; deuteration confirms a as 5-CH_3 (not shown). The short T_1's for the new peaks a′, b′ are emphasized in the WEFT ^{1}H NMR trace in Figure 4B, for which substantial intensity outside the solvent-obscured region is observed only for a′, b′; hence other peaks (if any) with similarly short T_1's must resonate in this obscured window, 3–6 ppm. Repeating the WEFT ^{1}H spectrum using perdeuterated imidazole-$^2H_4$ results in the trace in Figure 4C and confirms the origin of a′, b′ as the bound imidazole 2-H and/or 4-H, which are both very close to the iron. A similar trace using *1,2*-(^2H)$_2$-imidazole is shown in Figure 4D, which confirms that both a′, b′ arise from the bound imidazole 2-H. The two bound imidazoles in a bis complex are nonequivalent, and hence a′, b′ are the nonequivalent 2-H peaks, one from each ligand. The 4-H peak(s), which should have T_1's similar to 2-H,[39] must resonate in the 3–6 ppm window.

A direct ^{2}H NMR detection of PyropheoMEFe(Im-$^2H_4$)$_2^+$ (Figure 4E) yields relatively narrow lines for all nonlabile bound Im-$^2H_4$ peaks (paramagnetic influences are suppressed by $(\gamma(^2H)/\gamma(^1H))^2 \sim {}^1/_{43}$ and quadrupolar effects dominate[40]) and identifies the two single ^{2}H peaks a′, b′ (−11.0, −9.3 ppm), a peak c′ (~−2.0 ppm) of apparent double intensity of a′ or b′, and a shoulder, d′ (~2.0 ppm) to the solvent envelope. The peak c′ must be two nonlabile ^{2}H peaks from the bound Im-$^2H_4$ which are not strongly relaxed[39] by the iron in the undeuterated complex (Figure 4B) and hence must arise from two 5-^{2}H. This leaves d′, which is consistent with originating from 4-^{2}H.

High-Spin Complexes. Peak Assignments. The 360-MHz ^{1}H NMR spectrum of PyropheoMEFeCl in $(C^2H_3)_2SO$ is illustrated in Figure 5B. As in the case of hemin,[35] two sets of peaks, A_f

(37) The shifts at 25 °C are a (62.63), b (37.44), c (28.98), d (23.41), e (11.26), f (12.60), l (−0.94), m (−1.63), n (−1.89), p (−2.90), q (−3.24), r (−3.24), s (−4.54), t (−5.61), u (−5.80), v (−14.65), w (−15.93), in ppm from DSS.

(38) Inubushi, T.; Becker, E. D. *J. Magn. Reson.* **1983**, *51*, 128–133.

(39) Satterlee, J. D.; La Mar, G. N. *J. Am. Chem. Soc.* **1976**, *98*, 2804–2808.

(40) Balch, A. L.; La Mar, G. N.; Grazynski, L. L.; Renner, M. W.; Thanabal, V. *J. Am. Chem. Soc.* **1985**, *107*, 3003–3007.

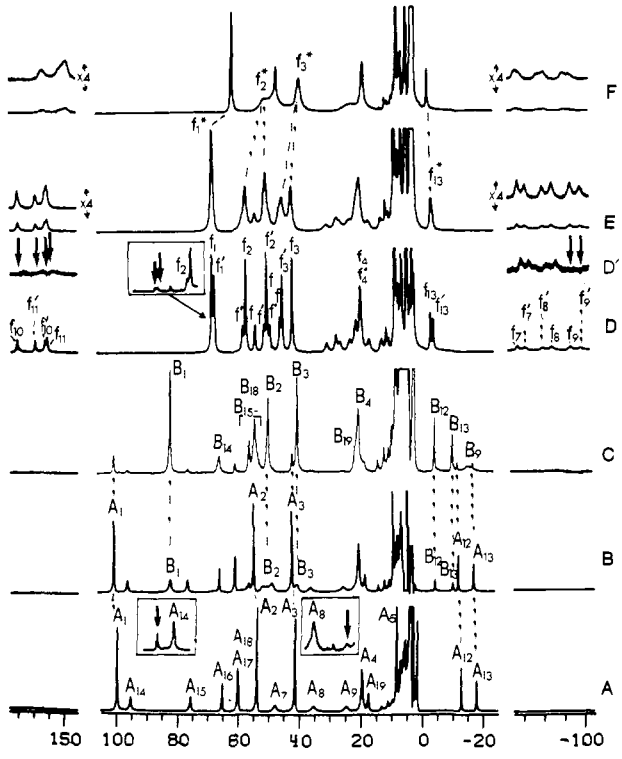

Figure 5. The 360-MHz ^{1}H NMR spectrum of (pyropheophorbide methyl ester)iron(III) chloride dissolved in $(C^2H_3)_2SO$ at 25 °C is shown in B. Two sets of resonances are detected labeled A_i and B_i (see text). Adding Ag^+ to precipitate chloride yields a sample giving rise to trace A with peaks A_i identified as due to the bis(DMSO) adduct. Inserts to trace A show the effect of deuteration which allows the assignment of peak A_1 as the 5-CH_3 and A_9 as the δ-meso-H; the γ-meso-CH_2 must resonate in the obscured window 2–8 ppm. The effect of addition of excess chloride to the sample giving rise to trace B is shown in C with peaks B_i. Similar deuteration allows the identification of peaks B_1 and B_9 as the 5-CH_3 and the δ-meso-H, respectively, and infers that the resonances due to the γ-CH_2 must be in the region obscured by the solvent (not shown). D shows the ^{1}H NMR spectrum of PyropheoMEFeCl in C^2HCl_3 at 25 °C. Two sets of peaks are observed: those arising from the major isomer are labeled f_i those relative to the minor component are labeled f'_i. The effect of deuteration is shown in trace D′ and in the inset box: peaks f_{10}, f_{11}, f'_{10}, f'_{11} are assigned to the γ-CH_2, peaks f_1, f'_1 to the 5-CH_3, and peaks f_9, f'_9 to the δ-meso-H. The addition of chloride leads to broadening of the lines and collapse f_1, f'_1 and f_{13}, f'_{13} to single peaks f_1* and f_{13}* (trace E). Complete averaging could be obtained for peaks in the 15–80 ppm region upon raising the temperature to 55 °C (trace F).

and B_i are observed, presumably from the chloride complex and from the bis(DMSO) adduct. Upon addition of $AgNO_3$ to precipitate Cl^-, the trace in Figure 5A is obtained, which exhibits only the one set of resonances, A_i, with 6 apparent methyl peaks A_1–A_6 (A_6 is on the shoulder of the intense diamagnetic signal; not shown) and 11 resolved single proton peaks (A_{17}, A_{18} are resolved on horizontal expansion, not shown). Thus only 15 of the expected 22 peaks are resolved outside the region 2–6 ppm. T_1 determination reveals the shortest T_1's (<1 ms) for A_7, A_8 A_9, indicating that they arise from the three meso-H's (Table II, supplementary material (see paragraph at the end of the paper)). The labeled sample with 5-C^2H_3, δ-meso-^{2}H, and γ-meso-C^2H_2 yields reduced intensity only for A_1 (5-CH_3) and A_9 (δ-meso-H) (inset to Figure 5A), dictating that γ-meso-CH_2 resonates in the 2–6 ppm window.

Attempts were made to assign peaks by NOEs at −25 °C in mixed DMSO/water solvent, as executed successfully for the low-spin complex. However, the only NOE that could be detected (~1%) was between A_{12} and A_{13} (not shown). Both the shifts and a detectable NOE thus suggest A_{12} and A_{13} are 2-vinyl H_β's.

The T_1 values of the five resolved methyls give a much shorter value for A_4, suggesting it arises from 8-CH_3 on the saturated pyrrole in **1**. A similarly attenuated contact shift and enhanced relaxation rate for the 3-methyl group on the saturated pyrrole B for the high-spin ferric sulfmyoglobin (containing **2**) has been reported.[9] The methyl peak A_5 likely arises from 4-β-CH_3, with A_2, A_3 hence attributable to 1-CH_3, 3-CH_3. The three narrower (~50 Hz) low-field single-proton peaks A_{16}–A_{18} likely arise from 2-H_α and 4-α-CH_2, as found in hemin models.[19,35] Thus the broader (80 Hz) two peaks A_{14}, A_{15} could arise from 7-H and 8-H on the saturated ring, since there are no other likely candidates on the unsaturated pyrroles based on porphyrin models.[19,35] The shift values, assignments, together with the T_1's and intercepts at $T^{-1} = 0$, are given in Table II (supplementary material).

Addition of excess Cl^- (in the form of tetraethylammonium chloride) to the solution giving rise to the trace in Figure 5B causes an increase in intensity and significant line narrowing (but not detectable change in shift) of the minor set of peaks B_i (Figure 5C). This chloride species exhibits three narrow low-field methyl peaks, B_1, B_2, B_3, a broad weakly shifted methyl peak, B_4 (overlapping a single-proton peak at this temperature), two narrow upfield single-proton peaks B_{12}, B_{13} (likely 2-vinyl H_βs), one broad upfield peak B_9, and five low-field single proton peaks B_{14}–B_{18} (B_{15}–B_{18} resolve at elevated temperature; not shown). The deuterium labeling reveals B_1 as 5-CH_3, γ-meso-CH_2 in the obscured region 3–8 ppm, and B_9 as δ-meso-H (not shown). Hence, the number and types of resonances for the two species giving rise to peaks A_i and B_i are very similar, except that the latter exhibits an upfield bias for the meso-H shifts. The chemical shifts are included in Table II (supplementary material).

The trace of PyropheoMEFeCl in C^2HCl_3 is illustrated in Figure 5D and exhibits spectral features dramatically different from those of the complexes in DMSO in the absence (Figure 5A) or in the presence (Figure 5C) of chloride ions. The trace does resemble[35] that of hemin chloride in C^2HCl_3 with the observation of strongly upfield shifted broad peaks associated with meso-H's. Also observed is an unprecedented set of strongly low-field-shifted peaks at 160–180 ppm. As is expected from the absence of any symmetry element for **1**, a five-coordinate complex would give rise to two isomers for chloride binding to the nonequivalent sides of the macrocycle. The peaks can be factored into two groups because the two isomers are not equally populated at 25 °C (~5:4 ratio), with the major and minor component peaks designated f_i and f_i', respectively. Isotope labeling reveals methyl peaks f_i and f_i' as 5-CH_3, broad upfield peaks f_9, f_9' as δ-meso-H, and low-field single proton peaks f_{10}, f_{11} and $f_{10'}$, $f_{11'}$ as γ-meso-CH_2. The remaining peaks can be assigned to pyrrole methyls (f_2, f_3 and f_2', f_3') and (tentatively) to pyrroline methyls (f_4, f_4', degenerate), and single proton peaks f_{13}, f_{13}' to a vinyl-H_β. Only the narrow single-proton peaks downfield of 30 ppm could be assigned to individual isomers by variable temperature studies. The shifts and available assignments are listed in Table III (supplementary material).

Dynamics of Chloride Exchange. Some information on the relationship between peaks for the two isomers of PyropheoMEFeCl in C^2HCl_3 could be obtained by taking advantage of our previous observation[41] that excess chloride induces "inversion" of the macrocycle via associative chloride exchange. Such exchange interconverts the two isomers and hence will lead to dynamic collapse of paired peaks f_i and f_i' (Figure 5F). Upon adding Cl^-, all lines tend to broaden, and certain ones collapse dynamically, as seen for f_1, $f_1' \rightarrow f_1$* and f_{13}, $f_{13}' \rightarrow f_{13}$* in Figure 5E. Upon further raising of the temperature of this sample to 55 °C, the collapse of methyls f_2, $f_2' \rightarrow f_2$* and f_3, $f_3' \rightarrow f_3$* can be induced. The collapse of the single proton peaks could not be followed uniquely. Other pairs of peaks are still in the slow-exchange limit because of the larger chemical shift difference between the isomers.

Analysis of the exchange contribution to the line width[41,42] of the collapsed set of peaks f_1, f_1' (5-CH_3, ~170 Hz) upon adding 8 equiv of Cl^- at 25 °C leads to an exchange rate ~10^2 s^{-1} and

(41) Snyder, R. V.; La Mar, G. N. *J. Am. Chem. Soc.* **1976**, *98*, 4419–4424.
(42) Sandström, J. *Dynamic NMR Spectroscopy*; Academic Press: London, 1982; Chapter 2.

to an expected second-order rate constant defined by rate = k_2[Cl][PyropheoMEFeCl], $k_2 \sim 10^6$ M^{-1} s^{-1}.

Discussion

Resonance Assignments. For the low-spin, dicyano complex, complete and unambiguous assignments were reached on the basis of partial deuterium labeling, spin decoupling, differential T_1 analysis, and NOEs. It should be noted, however, that while the first three types of data facilitated assignments, they were not essential and *all assignments could have been made solely on the basis of NOEs*. The detectability of the NOEs in such a small paramagnetic complex rests on the increased ^1H-^1H cross relaxation that occurs in viscous solvent.[30,31] Moreover, the NOEs not only provide assignment but also confirm the stereochemistry of **1**. Thus the ~3% NOE from 7-H (d) to 8-CH_3 (s) dictates that the two substituents are trans rather than cis about the saturated β-β bond. These NOE methods should be useful for structure elucidation for a variety of low-spin ferric chlorins.

Similar NOE experiments in viscous samples for the high-spin ferric complexes of **1** failed to yield useful assignments, most likely because of the much more efficient paramagnetic relaxation.[43] Qualitative comparison of T_1 data for the meso-H's indicates more rapid relaxation by a factor ~25 in the high-spin system. Thus even the larger NOEs (~20% for geminal protons) detected in the low-spin complex would be reduced to NOEs of <1%. The use of lower temperature to increase viscosity is counterproductive because of the onset of aggregation which causes additional line broadening.

Coordination Geometry. The fact that the final low-spin ^1H NMR spectrum of **1** is not achieved until 2 equiv of cyanide are added confirms the 2:1 ligation. Similarly, while an excess of Im is needed to completely form the low-spin complex with spectrum as in Figure 3A, the observation of two single-proton 2-H peaks a', b' (see above) confirms the bis(imidazole) ligation, as also found for analogous hemins.[20,39]

For the high-spin chloride complex of **1** in C^2HCl_3, the doubling of all peaks and the ability to interconvert the two species responsible for these peaks confirm the expected five-coordinate geometry, as found for ferric porphyrins.[35,44] When **1** is dissolved in DMSO in the absence of Cl^-, the NMR spectral parameters (low-field methyls and meso-Hs) are very similar to those of porphyrins[19,35] and dictate a six-coordinate bis(DMSO) structure, as found for porphyrins in both solution[45] and solid state.[46] For ferric porphyrins, addition of Cl^- in DMSO completely regenerated[35] the five-coordinate chloro complex with spectral properties indistinguishable from those of the five-coordinate complex in C^2HCl_3. In the presence of excess Cl^- in DMSO, however, **1** exhibits NMR (Figure 5C) and optical properties very distinct from those of the five-coordinate chloro complex in C^2HCl_3 (Figure 5D) but that do resemble more closely those of the bis(DMSO) complex (Figure 5A). Thus the chloro species of **1** in DMSO solution must have coordinated both chloride and DMSO. Because of the absence of a symmetry plane for **1**, two such monochloro, mono(DMSO) complexes are expected. However, with the large excess of both Cl^- and DMSO, there is likely facile interconversion between the isomers via ligand exchange.[41] Clear evidence for such an exchange process is observed in DMSO for low chloride concentration (Figure 5B), where the peak B_f exhibits considerable differential line broadening (depending on the shift difference in the two isomers) that is eliminated upon addition of excess Cl^- (Figure 5C) without changing shifts.

Comparison to Porphyrins. There exist in the literature few reports dealing with structural and/or dynamic properties that clearly differentiate porphyrins and chlorins in a manner that could bear on the role of chlorins in enzyme function.[13-15,22-24,47] Ligand affinities for strong-field ligands (CO) were found relatively insensitive to macrocycle saturation,[15] and only for some weak field ligands was a clear difference in ligand affinity noted.[13]

We find here that, while ferric porphyrins remain five-coordinated chloro complexes in DMSO, the present chlorin complex exists instead as a dominant six-coordinate monochloro, mono(DMSO) complex. Thus the ligand affinity for a sixth weak-field ligand is much stronger in chlorins than porphyrins. A similar trend for binding a fifth ligand to planar iron(II) chlorins has been reported.[13] This could result directly from the lower basicity of the chlorin relative to porphyrin or from the ability of the chlorin core to expand,[13,48] thereby allowing the iron to seat closer to the plane of the four nitrogens, which in turn favors binding a sixth ligand. Thus ferric porphyrins and chlorins appear to differ substantially in ligand affinities in the high-spin but not in the low-spin state.

The rate of "inversion" in five-coordinate ferric porphyrins, as induced by associative chloride exchange, has been studied in detail,[41] with second-order rate constants for the process in the range 10^2-10^3 M^{-1} s^{-1}, depending on the porphyrin. This rate constant appears to be some ~10^3 larger for the present chlorin, **1**. This significantly increased rate of "inversion" for chlorin relative to porphyrin is consistent with the relative ease with which chlorins can increase their core size, as discussed previously.[13]

Hyperfine Shift Patterns and π Bonding. Low-Spin Complexes. The hyperfine shifts, obtained by referencing the observed shift to that of a diamagnetic complex[49] of **1**, are also included in Table I. The hyperfine shifts for low-spin ferric porphyrins are known to consist of small-to-moderate (3-6 ppm) upfield dipolar shifts due to the magnetic anisotropy and larger contact shifts that are low downfield for core methyls and vinyl-H_α and upfield for vinyl-H_β's.[19-21] ESR data on low-spin ferric porphyrins and chlorins indicate[50] that the latter have significantly smaller magnetic anisotropy (range of g values), so it is highly probable that contact shifts similarly dominate in chlorin complexes.

For porphyrins, the contact shift has been shown to arise predominantly from spin delocalization[19-21] into the bonding $3e_\pi(xz)$ and $3e_\pi(yz)$ orbitals (more equally in models than in rhombically perturbed proteins[18,20]), as shown by the spin distribution[31] of Hückel MOs (see Figure 7A in ref 31). For a chlorin, the spin distribution for the related bonding π MOs,[31,51] S_6 and A_4, are available in Figure 7B of ref 31. The overall hyperfine shift pattern for **1** reveals large π contact shifts for substituents on pyrrole A (1-CH_3, 2-vinyl) and C (5-CH_3) and smaller upfield (most likely dipolar) shifts for the ring substituents on pyrrole B (3-CH_3, 4-ethyl). The $3e_\pi$ π MOs in a porphyrin and S_6, A_4 π MOs in a chlorin[31] are qualitatively similar, except that the unpaired spin is in the degenerate d_{xz}, d_{yz} orbitals in the former but is restricted to d_{xz} (and hence A_4) in the latter by the rhombic perturbation exerted by the ring D saturation.[20,31,52] One aspect of the apparent contact shift pattern in Table I that is not rationalized by the A_4, S_6 π bonding in **1** is the large low-field contact shifts for 7-H and 8-H.

It has been pointed out[16,17] that one of the major differences in metal π bonding to be expected in chlorins relative to porphyrins is that the former has a filled π MO (as in Figure 7B in ref 31) capable of and energetically ideally placed for π bonding, while

(43) Unger, S. W.; Lecomte, J. T. J.; La Mar, G. N. *J. Magn. Reson.* **1985**, *64*, 521-526.
(44) Koenig, D. F. *Acta Crystallogr.* **1965**, *18*, 663-673.
(45) Zobrist, M.; La Mar, G. N. *J. Am. Chem. Soc.* **1978**, *100*, 1944-1946.
(46) Hashiko, T.; Kastner, H. E.; Spartalian, K.; Scheidt, W. R.; Reed, C. A. *J. Am. Chem. Soc.* **1978**, *100*, 6354-6362.
(47) Stolzenberg, A. M.; Strauss, S. H.; Holm, R. H. *J. Am. Chem. Soc.* **1981**, *103*, 4763-4778.
(48) (a) Ullman, A.; Gallucci, J.; Fisher, D.; Ibers, J. A. *J. Am. Chem. Soc.* **1980**, *102*, 6852-6854. (b) Gallucci, J. C.; Swepston, P. N.; Ibers, J. A. *Acta Crystallogr.* **1982**, *B38* 2134-2139. (c) Kraty, C.; Angst, C.; Johansen, J. E. *Angew. Chem., Int. Ed. Engl.* **1981**, *20*, 211-212. (d) Spaulding, L. D.; Andrews, L. C.; Williams, G. J. B. *J. Am. Chem. Soc.* **1977**, *99*, 6918-6923. (e) Barkigia, K. M.; Fajer, J.; Spaulding. L. D.; Williams, G. J. B. *J. Am. Chem. Soc.* **1981**, *103*, 176-181.
(49) Katz, J. J.; Shipman, L. L.; Cotton, T. H.; Janson, T. R. *The Porphyrins* **1978**, *5*, 401-458.
(50) (a) Muhoberac, B. B.; Wharton, D. C. *J. Biol. Chem.* **1983**, *258*, 3019-3027. (b) Muhoberac, B. B. *Arch. Biochem. Biophys.* **1984**, *233*, 682-697.
(51) Gouterman, M. *The Porphyrins* **1979**, *4B*, 1-165.
(52) Shulman, R. G.; Karplus, M.; Glarum, S. H. *J. Mol. Biol.* **1971**, *57*, 93-115.

the analogous a_{1u} MO in the porphyrin is symmetry-restricted from such interaction with the iron. The characteristic spin distribution for this A_5 is large π spin density at the C_α's (near the ring junctions) of the saturated pyrrole D and smaller π spin density at the two adjacent meso positions.[31] For a normal, unsaturated pyrrole, π spin density at such a C_α position cannot be sensed directly[25] by any type of peripheral substituent. For the saturated pyrroline ring D, however, both 7-H and 8-H are α-protons[25] to the macrocycle C_α and are expected to exhibit low-field π contact shifts. Since no other π MO, either of $3e_\pi$ (A_4, S_6) or $4e_\pi^*$ (S_8^*, A_6^*) type places large π spin density[31] on C_α, the observed large low-field contact shifts for 7-H and 8-H are *direct evidence for important π metal bonding involving A_5, derived from the a_{1u} of a porphyrin.* An estimate for the spin density, ρ_π, at C_α of ring D is obtainable from the relationship between contact shift,[25] δ_{con}, and ρ_π, via $\rho = \delta_{con}K/Q_0 \cos^2 \phi$, where ϕ is the angle between the C_α p_z axis and the C_α–C_β–H plane, $Q_0 \sim 140$ MHz, and $K = 4.2 \times 10^4$ MHz/ppm for low-spin iron(III) at 25 °C. For 7-H and 8-H, $\delta_{con} \sim 20$ ppm, $\phi \sim 90°$, leading to $\rho_\pi(C_\alpha) \sim 6 \times 10^{-3}$ spin. The significance of this spin density for defining the degree of π bonding between the iron and A_5 π MO must await more sophisticated molecular orbital calculations involving the iron.

The observed shifts for the axial imidazole in the bis(imidazole) complex of **1** differ from those in the analogous porphyrin complex[19,39] in that they tend to show an upfield bias in the former relative to the latter complex. However, the axial imidazole shifts are known to have a large downfield dipolar contribution in ferric porphyrins, so that the upfield bias in the present chlorin is consistent with the reduced magnetic anisotropy in chlorins without involving important changes in axial π bonding.

High-Spin Complexes. All three characterized high-spin complexes of **1** exhibit only three core methyls with contact shifts comparable to those observed for all four methyls in porphyrins.[19,35] The fourth methyl exhibits strongly attenuated contact shift and enhanced paramagnetic relaxation and is assigned to 8-CH_3 on the saturated pyrrole D. The basis for this assignment is that for **2** in a high-spin ferric protein, only 3-CH_3 exhibits similarly reduced contact shift and increased relaxation rate, as determined by isotope labeling.[9]

For the six-coordinate bis(DMSO) complex, the dominant contact shift pattern is generally similar to that observed for six-coordinate ferric porphyrins,[19,35] with low-field shifts for all substituents except vinyl-H_β. Note particularly the absence of significant contact shifts for γ-meso-CH_2. This pattern of contact shifts has been interpreted to arise from a combination of σ spin delocalization with some π spin density in the filled $3e_\pi$ in a porphyrin[19,21] (and hence A_4, S_6 in a chlorin).[31] The small low-field meso-H and negligible γ-meso-CH_2 contact shifts argue against significant π spin density in the lowest vacant π MO ($4e_\pi^*$ in porphyrin, A_6^*, S_8^* in chlorin).[31] The inability to assign low-field single-proton peaks (and hence identify 7-H, 8-H) precludes any interpretation of the role of A_5 in π spin delocalization.

For the five-coordinate chloro complex of **1**, the shifts for three methyls are similar to those in porphyrins.[19,35] Moreover, while the meso-H shifts are upfield, the shifts are substantially larger than for porphyrins. These upfield meso-H shifts have been interpreted[19,21] as direct evidence for Fe → P π back-bonding into $4e_\pi^*$ and hence can be interpreted in terms of such π bonding into S_8^* and A_6^* for chlorins. For the present ferric chlorin, the evidence for such π bonding is even more compelling, since we observe both large upfield meso-H and large downfield γ-meso-CH_2 contact shifts in the same complex.[19,25] It is also noted that the magnitude of the contact shifts are larger for δ-meso-H ($\sim$ +100 ppm) and γ-meso-CH_2 ($\sim$−170 ppm) than the α-meso-H and β-meso-H. While A_6^* and S_8^* make no such specific predictions[31] (in fact, the opposite is suggested[31] by both A_6^*, S_6^*) this pattern is consistent with π spin density in A_5 for which the dominant spin density is at pyrrole D C_α's and the adjacent γ- and δ-meso positions. Thus both high-spin and low-spin ferric chlorin complexes support important contributions from π bonding with A_5.

Comparison to Other Ferric Chlorins. The only ferric chlorin system for which detailed NMR assignments have been carried out are the sulfmyoglobins[9] and the extracted sulfhemin prosthetic group from the terminal alkaline equilibration product of sulfmyoglobin,[31] **2**. Characteristic for the high-spin forms of both **1** and **2** is the sharp attenuation of the contact shift of one methyl, which for **2** could be established to originate from the saturated pyrrole B. While this argues for assigning peaks A_4 (and B_4, f_4, f_4') to 8-CH_3 for **1**, experimental confirmation is lacking.

For the low-spin ferric complexes, the π contact shift patterns for **1** and **2** agree remarkably in two respects. Firstly, in both cases the saturated pyrrole induces a rhombic perturbation that places the lone unpaired spin[31] into the iron d_{xz} orbital which delocalizes spin density into A_4 but not S_6. Hence the orbital ground state for low-spin ferric chlorins may be generally determined by the site of the ring saturation and is not altered by incorporation into a protein matrix.[9,31,52] Secondly, in each case the π spin density on the pyrroles adjacent to the saturated ring (i.e., pyrroles A and C for both **1** and **2**) exhibits large asymmetry, with the positions adjacent to the saturated ring (5-CH_3 and 2-vinyl for **1**, 1-CH_3 and 6-α-CH_2 for **2**) exhibiting much larger contact shifts than the neighboring position on that pyrrole (1-CH_3 for **1**, 2-vinyl and 5-CH_3 for **2**). This subtlety in the π spin distribution is not apparent in the crude Hückel π MO predictions.[31] It is possible that this asymmetry in π spin density in the two pyrroles adjacent to the saturated ring may be a general characteristic of low-spin ferric chlorin complexes and hence can provide a model for interpreting the NMR properties of low-spin ferric chlorin enzymes.

Thus the low-spin nitrite complex of the bovine spleen green heme protein exhibits[4] an ^1H NMR spectrum for which the largest low-field contact shifts are observed for a pair of single protons ($\sim$40, $\sim$46 ppm) and one methyl group ($\sim$33 ppm). If the chlorin prosthetic group in this enzyme[3] is based on the protoporphyrin IX skeleton, as is the case for **1** and **2**, then the largest contact shifts would be expected (for a given site of pyrrole saturation) as follows: 4-H_α, 7-α-CH_2 (ring A) 1-CH_3, 6-α-CH_2 (ring B) 1-CH_3, 8-CH_3 (ring C) or 2-H_α, 5-CH_3 (ring D). Thus the observation of a single strongly shifted methyl argues strongly against saturation sites at ring A or C, which predict either no methyls or two methyls with large contact shifts. Differentiation between ring B or D saturation is complicated by the fact that the core protons on the saturated ring (i.e., 7-H, 8-H for **1**) can also display large low-field contact shifts. If, however, NOE studies on the enzyme can confirm that the strongly shifted single protons are geminal partners, this would support solely ring B as the saturated pyrrole.

It is noted that the previous ^1H NMR analysis of the low-spin ferric complex of the sulfhemin chlorin, **2**, failed to provide[31] any evidence for π spin density in A_5. However, the spin density in this π MO of a chlorin is optimally detected only by hydrogens directly attached to the saturated ring core,[25] and such probes were absent in the sulfhemin complexes.

Acknowledgment. We are indebted to A. L. Balch, J. Fajer, L. H. Hanson, and S. E. Strauss for valuable discussions. S.L. acknowledges the support of the C.N.R. (Italy) for a research fellowship. This research was supported by grants from the National Institutes of Health, GM-26226 and HL-22252.

Supplementary Material Available: Figure 2 showing ^1H NMR spin decoupling of dicyanopyropheophorbide *a* methyl ester and Tables II and III showing ^1H NMR spectral parameters for the high-spin complexes (3 pages). Ordering information is given on any current masthead page.